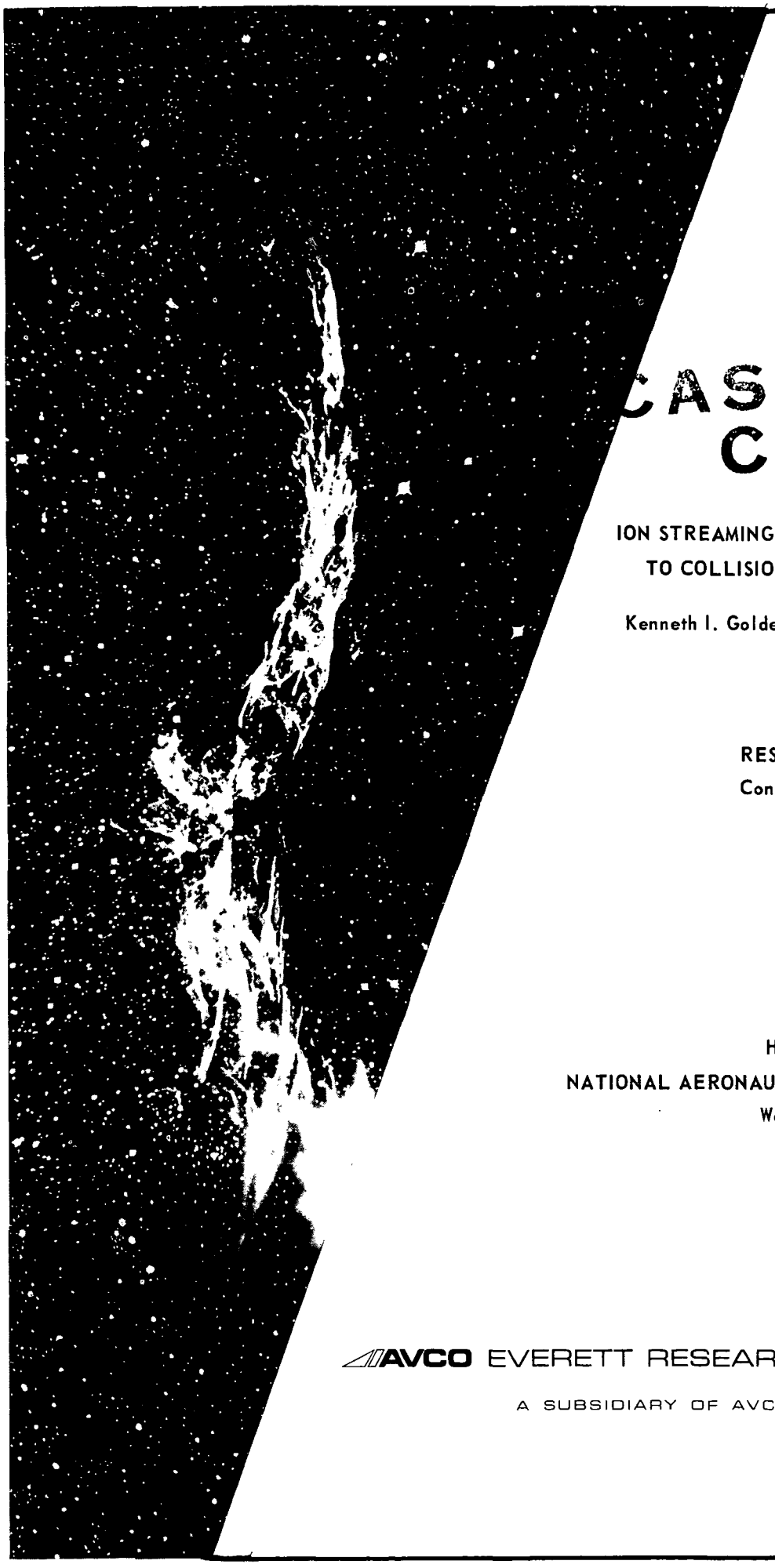



# ION STREAMING INSTABILITIES WITH APPLICATION TO COLLISIONLESS SHOCK WAVE STRUCTURE

Kenneth I. Golden, Lewis M. Linson and Siva A. Mani

RESEARCH REPORT 383
Contract No. NASW–2302
March 1973

prepared for

HEADQUARTERS
NATIONAL AERONAUTICS AND SPACE ADMINISTRATION
Washington, D. C.

AVCO EVERETT RESEARCH LABORATORY, INC.
A SUBSIDIARY OF AVCO CORPORATION

RESEARCH REPORT 383

# ION STREAMING INSTABILITIES WITH APPLICATION TO COLLISIONLESS SHOCK WAVE STRUCTURE

by

Kenneth I. Golden,* Lewis M. Linson** and Siva A. Mani

AVCO EVERETT RESEARCH LABORATORY, INC.
a Subsidiary of Avco Corporation
Everett, Massachusetts

Contract No. NASW-2302

March 1973

prepared for

HEADQUARTERS
NATIONAL AERONAUTICS AND SPACE ADMINISTRATION
Washington, D. C.

* Permanent address: Department of Electrical Engineering, Northeastern University, Boston, Massachusetts 02115

** Present address: Science Applications, Inc., LaJolla, California 92037

Page Intentionally Left Blank

## ABSTRACT

The electromagnetic dispersion relation for two counterstreaming ion beams of arbitrary relative strength flowing parallel to a dc magnetic field is derived. The beams flow through a stationary electron background and the dispersion relation in the fluid approximation is unaffected by the electron thermal pressure. Magnetic effects on the ion beams are included but the electrons are treated as a magnetized fluid, $m_e \to 0$. The dispersion relation is solved with a zero net current condition applied and the regions of instability in the k-U space (U is the relative velocity between the two ion beams) are presented. These results are extensions of Kovner's analysis for weak beams. The parameters are then chosen to be applicable for parallel shocks. We find that unstable waves with zero group velocity in the shock frame can exist near the leading edge of the shock for upstream Alfven Mach numbers greater than 5.5. It is suggested that this mechanism could generate sufficient turbulence within the shock layer to scatter the incoming ions and create the required dissipation for intermediate strength shocks.

Page Intentionally Left Blank

TABLE OF CONTENTS

## INTRODUCTION

The instabilities that result from the presence of two interpenetrating ion streams immersed in an electron background may provide the mechanism for collisionless momentum coupling between the two streams. The presence of a weak magnetic field can have a significant effect on the physical process. First, gradients in the magnetic field give rise to electron currents that can drive ion acoustic waves unstable and increase the effective collision frequency;[1,2] second, when the propagation is perpendicular to the magnetic field,[3-6] the magnetic field can inhibit the electrons from shorting out ion plasma oscillations for wavelengths long compared to the electron gyroradius; and third, whistler mode-ion beam interactions are likely to be important, and the existence of whistler modes depends on the presence of a magnetic field. It is this third aspect, and in particular, its application to collisionless oblique and parallel shock wave structures, that is of interest in this paper.

Significant among recent advances in magnetic streaming instabilities and their applications to collisionless oblique shock wave structures are the so-called "beam-cyclotron" (BC)[7,8] and "beam-whistler" (BW)[9] instabilities. These are characterized by possible interaction between one of the two counterstreaming ion acoustic beam modes and the electron cyclotron or whistler mode (Fig. 1). While the BC instability does result in electron heating, it nevertheless may be

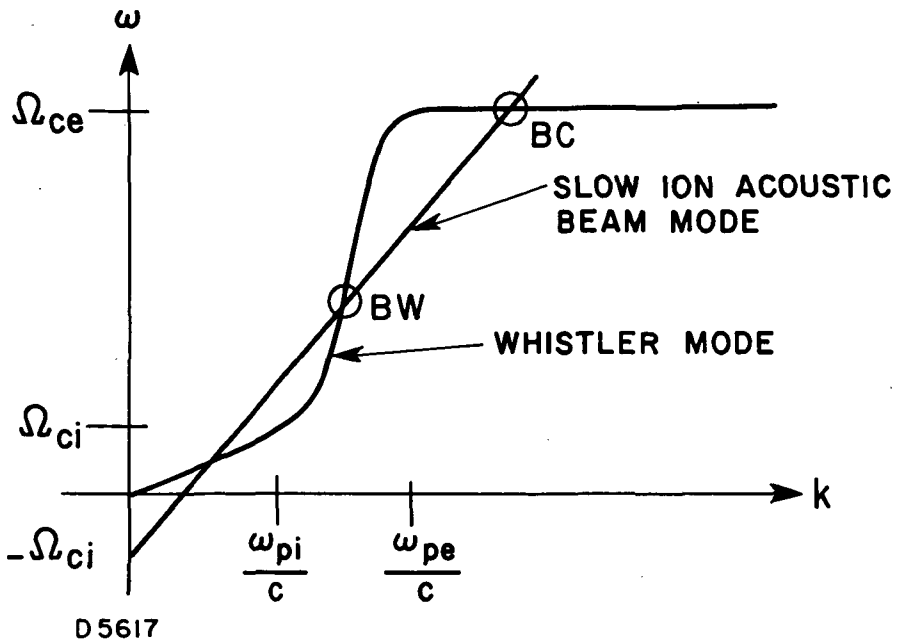


Fig. 1 Schematic of the Dispersion Relation Showing the Interaction Regions Leading to Beam-Cyclotron (BC) and Beam-Whistler (BW) Instabilities.

inadequate as a mechanism for ion-ion momentum coupling, for this instability can be stabilized by electron heating or by resonance broadening or by ion trapping.[7] On the other hand, BW instabilities do result in turbulence which can suitably couple the two ion beams. The application of BW interactions to collisionless shock structures is especially attractive since they are found to be operative over a substantially larger range of Mach numbers than are the so-called "magnetic counter-streaming ion-ion"[3-4] and "modified"[5,6] two stream instabilities associated with perpendicular shocks.

It is interesting to note that for parallel propagation ($\underset{\sim}{k} \parallel \underset{\sim}{B}_o$) the ion acoustic modes of the counterstreaming ions uncouple from the whistler mode in the linear BW dispersion relation cited by Biskamp and Welter.[9] Thus, in their assumed frequency range $\Omega_{ci} \ll |\omega| \ll \Omega_{ce}$ ($\Omega_{ci}$ and $\Omega_{ce}$ being the ion and electron cyclotron frequencies), the whistler modes are stable. On the other hand, if one relaxes the frequency restriction to lower frequencies, i.e., $0 < |\omega| \ll \Omega_{ce}$, then, even in the case of parallel propagation, a beam mode can, in fact, enter into unstable interaction with the whistler leading to coupling of the two ion beams. The object of this paper is to analyze this instability especially for parameters that can be related to parallel shocks.

In Section II we present an analysis of the whistler mode instability arising in a collisionless plasma configuration consisting of two ion beams counterstreaming along the magnetic field in the rest frame of the background electrons. In Section III we shall determine when these unstable whistler modes can grow to large amplitude inside a

shock front propagating along the magnetic field. These calculations are carried out in the shock frame at different upstream Mach numbers and at different stations within the shock thickness. The result of these calculations is a map showing the range of Mach numbers as a function of position into the shock for which unstable whistlers can stand inside the shock. A summary of the results is presented in Section IV.

## LINEAR ANALYSIS

We consider an unbounded collisionless plasma consisting of two ion beams of densities $n_1$ and $n_2$ counterstreaming with velocities $\underset{\sim}{V}_1$ and $\underset{\sim}{V}_2$ parallel to a steady magnetic field $\underset{\sim}{B}_o$ taken to lie along the positive z-axis. We assume the background electrons to be at rest. The charge neutrality and zero current conditions give

$$n_1 + n_2 = n_e \tag{1}$$

and

$$n_1 \underset{\sim}{V}_1 + n_2 \underset{\sim}{V}_2 = 0 \tag{2}$$

where $n_e$ is the number density of electrons. For the low frequency case that we are interested in, it is crucial that the zero current condition (2) be met for arbitrary values of the beam strength[10] ($0 \leq n_2/n_e \leq 1$). The electron motions are modeled by fluid equations which are valid for wavelengths long compared with the electron gyroradius while the ions are assumed to be cold. The dielectric tensor for such a plasma is easily calculated and the appropriate electromagnetic streaming dispersion relation for plane waves exp [i ($\underset{\sim}{k} \cdot \underset{\sim}{r}$ - $\omega t$)] for the case of parallel propagation ($\underset{\sim}{k} \parallel \underset{\sim}{B}_o$) takes the form

$$k^2 c^2/\omega^2 - \epsilon_{xx}(\underset{\sim}{k}, \omega) = \pm i \epsilon_{xy}(k, \omega) \tag{3}$$

where

$$\epsilon_{xx}(\underset{\sim}{k}, \omega) = 1 - \frac{\omega_{pe}^2}{\omega^2 - \Omega_{ce}^2} - \sum_{s=1}^{2} \frac{(\omega_{ps}^2/\omega^2)(\omega - \underset{\sim}{k}\cdot \underset{\sim}{V}_s)^2}{(\omega - \underset{\sim}{k}\cdot \underset{\sim}{V}_s)^2 - \Omega_{ci}^2}$$

$$\epsilon_{xy}(\underset{\sim}{k}, \omega) = \frac{i\Omega_{ce}\omega_{pe}^2}{\omega(\omega^2 - \Omega_{ce}^2)} - \sum_{s=1}^{2} \frac{i\Omega_{ci}(\omega_{ps}^2/\omega)^2(\omega - \underset{\sim}{k}\cdot \underset{\sim}{V}_s)}{(\omega - \underset{\sim}{k}\cdot \underset{\sim}{V}_s)^2 - \Omega_{ci}^2}$$

and $k = |\underset{\sim}{k}|$ .

In the above, $\omega_{ps} = (4\pi n_s e^2/m_i)^{1/2}$ and $\omega_{pe} = (4\pi n_e e^2/m_e)^{1/2}$ are the s th ion beam (s = 1, 2) and electron plasma frequencies respectively. We note that within the fluid approximation, the dispersion relation (3) is unaffected by electron thermal effects for the case of parallel propagation.

We now make the low frequency approximations that the displacement current is negligibly small ($\omega \ll kc$) and that the electrons have zero mass ($|\omega| \ll \Omega_{ce}, \omega_{pe}$). Introducing the dimensionless beam density $\eta = n_2/n_e$ and $\omega_{pi}^2 = \Sigma \omega_{ps}^2$, the dispersion relation (3) simplifies to

$$\frac{k^2c^2}{\omega_{pi}^2} \mp \frac{\omega}{\Omega_{ci}} + \frac{(1-\eta)(\omega - \underset{\sim}{k}\cdot \underset{\sim}{V}_1)}{\omega - \underset{\sim}{k}\cdot \underset{\sim}{V}_1 \pm \Omega_{ci}} + \frac{\eta(\omega - \underset{\sim}{k}\cdot \underset{\sim}{V}_2)}{\omega - \underset{\sim}{k}\cdot \underset{\sim}{V}_2 \pm \Omega_{ci}} = 0 \qquad (4a, b)$$

where Eq. (4a) refers to the upper signs and Eq. (4b) refers to the lower signs. In what follows, Eq. (4b) corresponding to the lower sign will be dropped from further consideration since its solution can be recovered from that of Eq. (4a) by the substitutions $\omega \to -\omega$ and $\underset{\sim}{k} \to -\underset{\sim}{k}$. It is convenient at this point to introduce the relative drift velocity $\underset{\sim}{U} = \underset{\sim}{V}_2 - \underset{\sim}{V}_1$, so that we have $\underset{\sim}{V}_1 = -\eta\underset{\sim}{U}$ and $\underset{\sim}{V}_2 = (1-\eta)\underset{\sim}{U}$ where use has been made of the zero current condition (2). With these substitutions Eq. (4a) simplifies to

$$\frac{k^2c^2}{\omega_{pi}^2} - \frac{\omega}{\Omega_{ci}} + 1 - \frac{(1-\eta)\Omega_{ci}}{\omega + \eta\, \underset{\sim}{k}\cdot\underset{\sim}{U} + \Omega_{ci}} - \frac{\eta\,\Omega_{ci}}{\omega - (1-\eta)\, \underset{\sim}{k}\cdot\underset{\sim}{U} + \Omega_{ci}} = 0 \quad (5)$$

Now, for $0 \leq \eta \leq 0.5$, it is clear that the ion stream 1 has more the role of "plasma" while 2 has more the role of "beam." When $0.5 \leq \eta \leq 1$, these roles are interchanged. However, as the interchanges

$$\eta \longleftrightarrow (1-\eta) \quad , \quad \underset{\sim}{k}\cdot\underset{\sim}{U} \longleftrightarrow -\underset{\sim}{k}\cdot\underset{\sim}{U}$$

leave Eq. (5) unchanged, the analysis of the range $0.5 \leq \eta \leq 1.0$ would be redundant. It therefore suffices to investigate the range $0 \leq \eta \leq 0.5$. For $\eta = 0$, we recover the usual whistler ($W\pm$) and ion-cyclotron dispersion branches given analytically by

$$\omega_{\pm} = k^2C_A^2/2\Omega_{ci} \pm kC_A\,(1 + k^2C_A^2/4\Omega_{ci}^2)^{1/2} \quad (6)$$

where $C_A = (B_o^2/4\pi m_i n_e)^{1/2}$ is the Alfven speed. For weak beams ($\eta \ll 1$), the intersection points P, Q, R (see Fig. 2) between the ion beam mode

$$\omega = (1-\eta)\, \underset{\sim}{k}\cdot\underset{\sim}{U} - \Omega_{ci} \quad (7)$$

and the $W_+$ and $IC_-$ branches of (6) suggest possible strong interactions near these points. Indeed Kovner's analysis[11] shows that the beam-$IC_-$ interaction is stable while the beam - $W_+$ interactions are unstable with growth rates

$$\text{Im}\ \omega_\ell = \frac{\eta^{1/2}\,\Omega_{ci}k_\ell U}{(k_\ell^2 U^2 - \Omega_{ci}^2)^{1/2}} \qquad (\ell = P, Q),$$

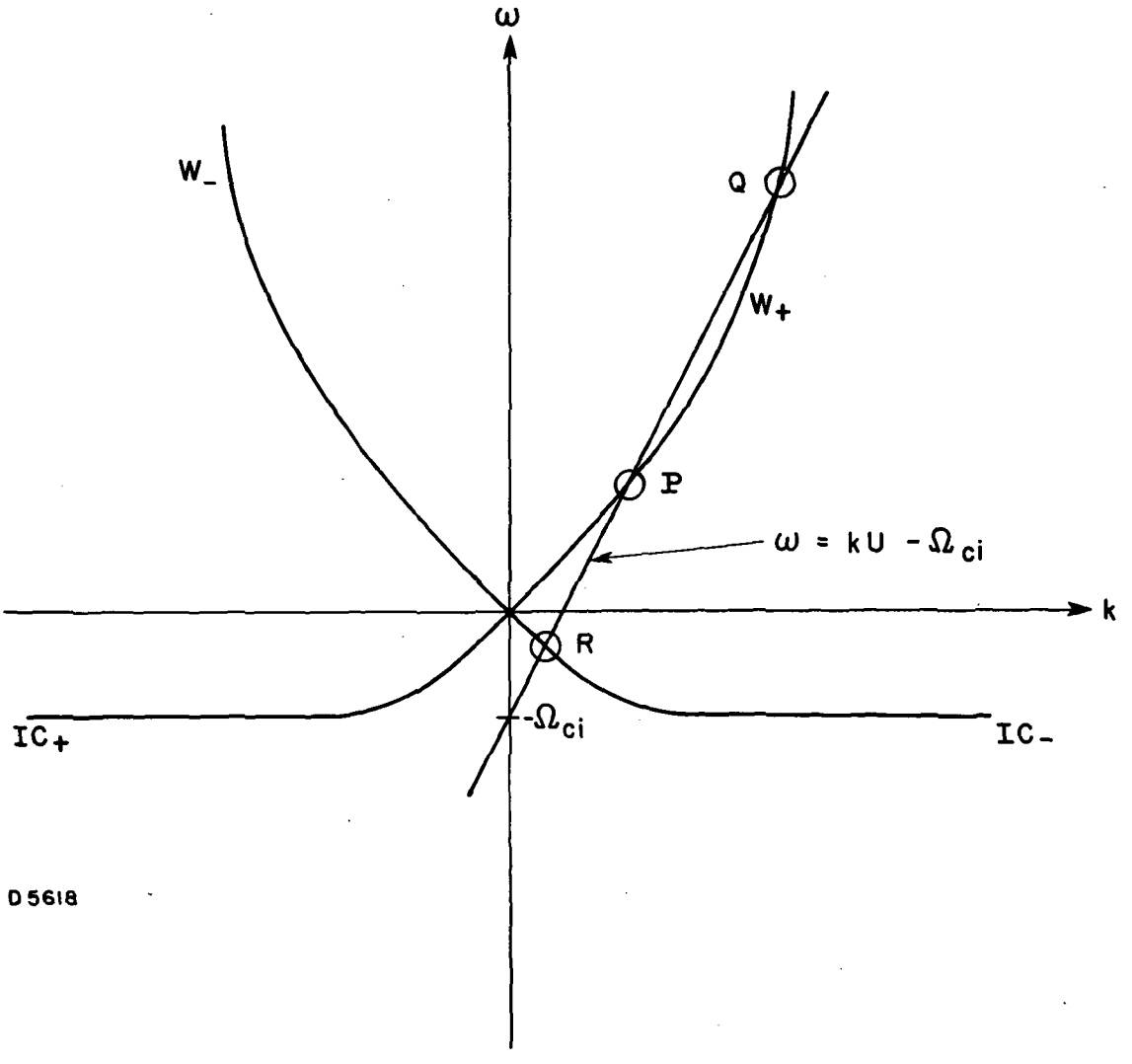


Fig. 2 Superposition of the Whistler ($W_+$) and Ion Cyclotron ($IC_+$) Modes for $\eta = 0$ With a Weak Beam Mode. The intersection points R, P, and Q represent regions where strong interactions can occur.

where, from (6) and (7), $k_P$ and $k_Q$ depend on the slope ($= U/C_A$) of the beam line. We note that the beam-cyclotron (BC) intersection shown in Fig. 1 does not appear in Fig. 2 due to our approximation $m_e \to 0$.

We have extended Kovner's weak beam study by solving (5) for arbitrary values of $\eta$ and drift Mach number $M_d = U/C_A$. By expanding the dispersion relation (5) for small k, one readily finds

$$\text{Im } \omega = k\, C_A \left[\eta\,(1 - \eta)\, M_d^2 - 1\right]^{1/2},$$

so that these long wavelength modes are unstable only if

$$M_d > \frac{1}{\left[\eta\,(1 - \eta)\right]^{1/2}} \tag{8}$$

This condition is thus sufficient for instability, but is not necessary as we shall see below. We should emphasize that due to the application of the condition (2), we are dealing only with zero-current instabilities and thus the stronger, current-driven instabilities often treated are excluded.

The dispersion curves and growth spectrum from (5) are plotted in Figs. 3a, b, c and d for values of $\eta = 0.1$ and $0.5$ and $M_d = 3$ and 7. In plotting these, kU has been taken to be negative with a view to the application in the shock problem discussed in the following section. We find that for $\eta = 0.1$, the peak growth rate $\omega''$ ($\omega = \omega' + i\omega''$) increases only slightly from $\omega'' \simeq 0.32\ \Omega_{ci}$ at $M_d = 3$ to $\omega'' \simeq 0.38\Omega_{ci}$ at $M_d = 7$. For $\eta = 0.5$, the peak growth rate increases more markedly with $M_d$, rising from $\omega'' \simeq 0.34\Omega_{ci}$ at $M_d = 3$ to $\omega'' \simeq 0.72\Omega_{ci}$ at $M_d = 7$. For $\eta = 0.5$, the dispersion curves are symmetric in k as it is impossible to distinguish the beam

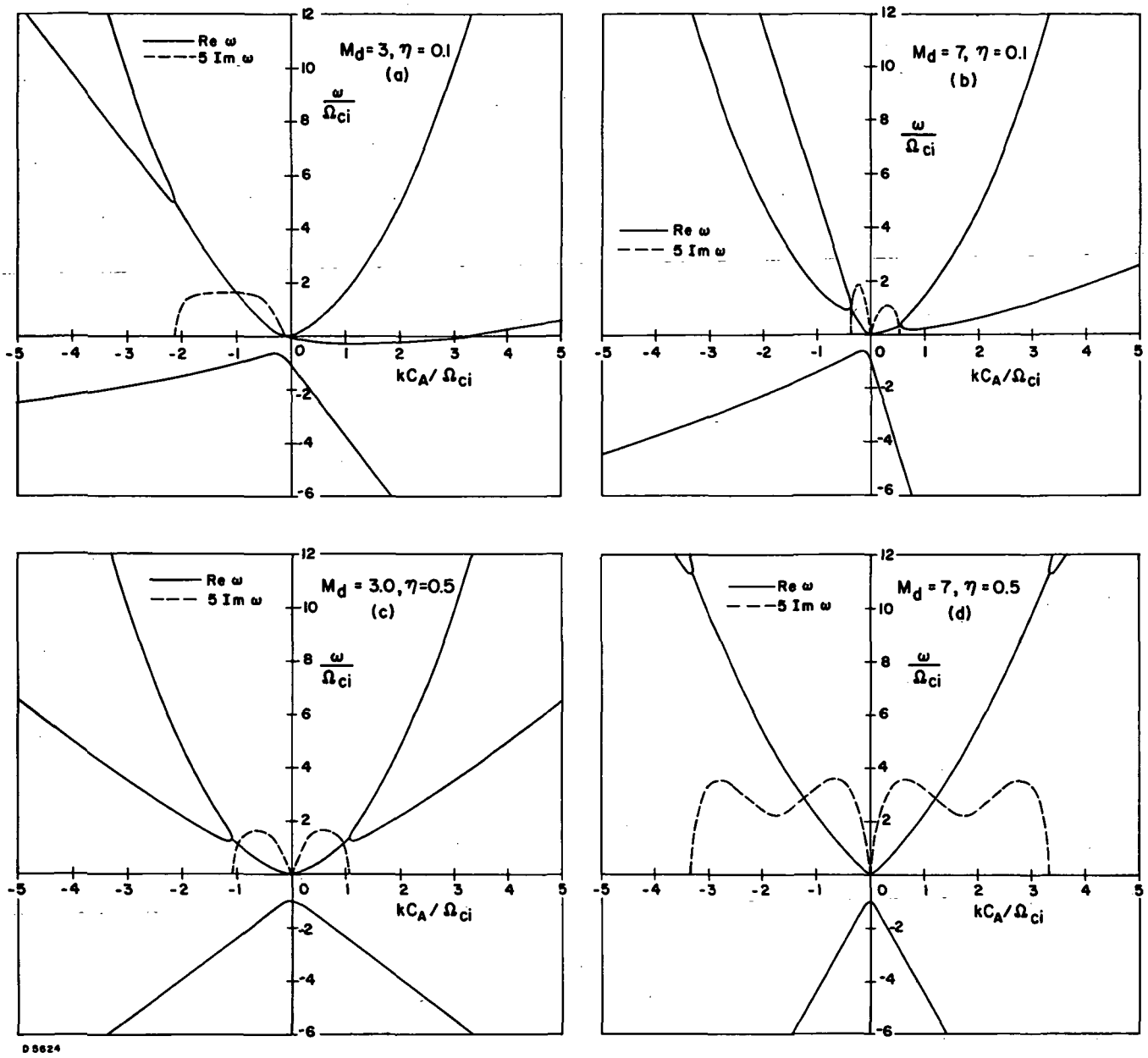


Fig. 3 The Dispersion Relation (5) for: a) $\eta = 0.1$, $M_d = 3$, b) $\eta = 0.1$, $M_d = 7$; c) $\eta = 0.5$, $M_d = 3$; d) $\eta = 0.5$, $M_d = 7$. Note that the vertical scale should be multiplied by 1/5 in order to obtain the correct value for Im $\omega$.

from the plasma while for $\eta = 0.1$, the beam-like mode can be clearly identified. We also note that in Fig. 3a the region near $k = 0$ is stable in agreement with (8) but that there is instability for a finite range of negative k.

The regions of instability in k - U space for $\eta = 0.1$ and 0.5, obtained by setting the discriminant of the cubic equation (5) equal to zero, are shown in Figs. 4a and 4b respectively. Also shown by dashed lines is the generalization for arbitrary $\eta$ of the Kovner lines. These lines give the values of k and U (for a given $\eta$) that simultaneously satisfy (6) and (7) and correspond to the intersection points P and Q in Fig. 2. It is easy to show that the Kovner lines always lie in the region of instability and that they have a minimum at $kC_A/\Omega_{ci} = (4/3)^{1/2} \simeq 1.15$ for which $M_d \simeq 2.6/(1-\eta)$. This value corresponds to the relative drift such that the beam line in Fig. 2 is tangent to the $W_+$ branch, i.e., the points P and Q coalesce.

For large drift ($M_d \to \infty$) there are unstable modes for k in the range

$$\left| (1-\eta)\, M_d - \frac{2}{M_d(1-\eta^{1/2})} \right| < \left| \frac{kC_A}{\Omega_{ci}} \right| < \left| (1-\eta)\, M_d - \frac{2}{M_d(1+\eta^{1/2})} \right| .$$

The width of this unstable spectrum is thus

$$\Delta k \simeq \frac{4\eta^{1/2}}{(1-\eta)U}\ \Omega_{ci} \qquad (9)$$

and the peak growth rate is approximately given by $\omega'' \simeq \eta^{1/2}\, \Omega_{ci}$. These expressions are in agreement with the numerical results shown in Figs. 3 and 4.

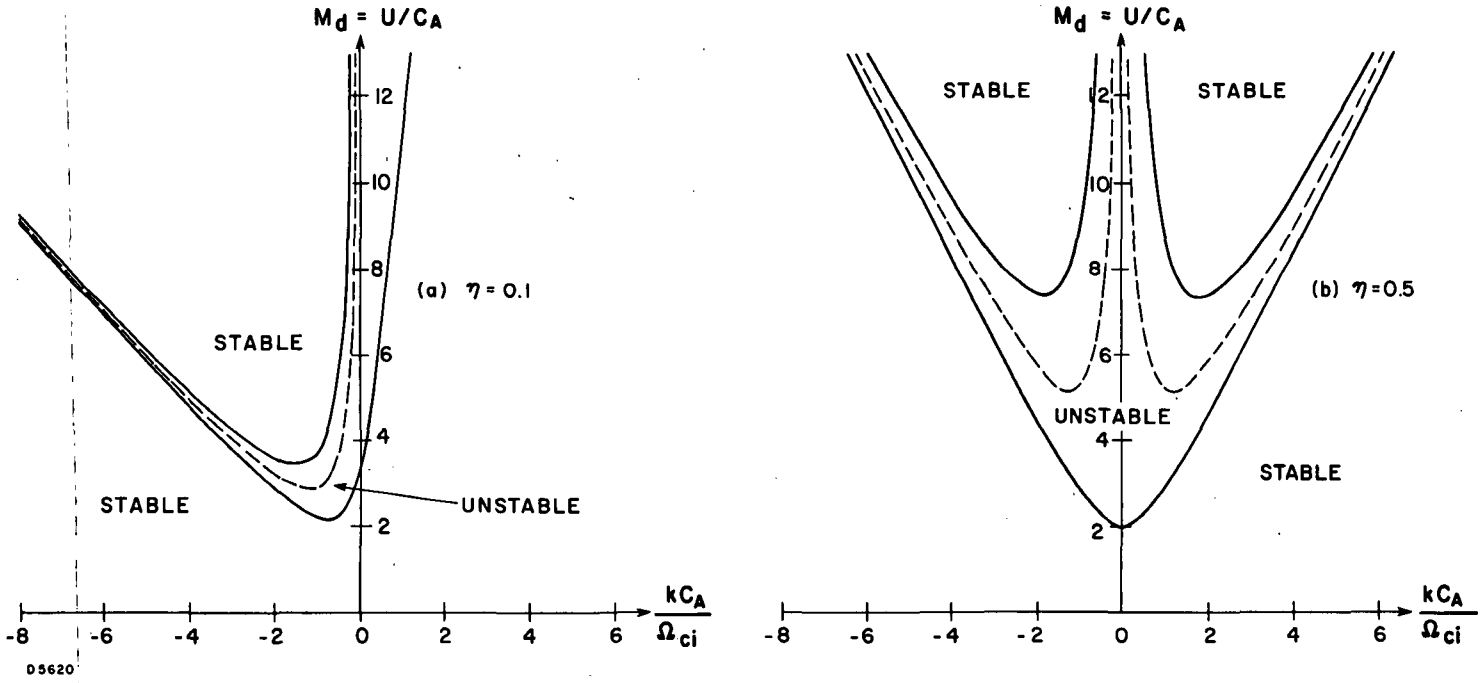


Fig. 4 Range of Unstable Values of k as a Function of Relative Drift Velocity for a) $\eta = 0.1$ and b) $\eta = 0.5$.

## APPLICATION TO SHOCK WAVE STRUCTURE

The origin of the magnetic field turbulence associated with collisionless shock waves has not been definitely established. If the instability discussed in the preceding section has relevance for parallel shock wave structure, then the unstable waves must be able to grow to large amplitude inside the shock front. This requirement suggests that the phase or group velocity of the whistler in the shock frame should be either zero or very small in addition to the wave being unstable. Wave packets with zero group velocity can be expected to remain in the shock front for a sufficiently long time to reach large amplitude and generate turbulence. In the present work, we consider only parallel shock waves for which the sound speed $C_{S0} = (\gamma\kappa(T_e + T_i)/m_i)^{1/2}$ and the Alfven speed $C_{A0}$ in the unshocked gas are equal. The external magnetic field in this case remains constant and parallel to the direction of plasma flow across the shock layer. We thus exclude any consideration of "switch-on" shocks [12] that occur for $C_{S0} < C_{A0}$.

We adopt the Mott-Smith formalism which supposes that the shock layer is already a two-streaming environment for the ions. Therefore the ion distribution function in the rest frame of the shock front is assumed to be a linear combination of the upstream (u) and downstream (d) velocity distribution functions, i. e.,

$$f_i(z, \underset{\sim}{v}) = n_u(z)\ \delta(\underset{\sim}{v} - \underset{\sim}{V}_u) + n_d(z)\ \delta(\underset{\sim}{v} - \underset{\sim}{V}_d). \tag{10}$$

For simplicity, we take $n_u(z)$ to decrease linearly from the upstream value at the leading edge of the shock to zero at the trailing edge while we assume $n_d(z)$ to increase linearly from zero at the leading edge to its downstream value at the trailing edge. A schematic of the density and velocity distributions is sketched in Fig. 5. The electrons, on the other hand, are treated as a single fluid moving with an average drift velocity, $\underset{\sim}{V}_e(z)$, determined by the zero current condition

$$\begin{aligned} \underset{\sim}{V}_e(z) &= \frac{n_u(z)}{n_e(z)} \underset{\sim}{V}_u + \frac{n_d(z)}{n_e(z)} \underset{\sim}{V}_d \\ &= [1 - \eta(z)] \underset{\sim}{V}_u + \eta(z) \underset{\sim}{V}_d \end{aligned} \tag{11}$$

where the fraction of the total density represented by the downstream species $\eta(z)$ is now a function of position through the shock.

The appropriate dispersion relation is easily obtained from (5) by doppler shifting the frequency $\omega$ by the amount $\underset{\sim}{k} \cdot \underset{\sim}{V}_e(z)$ which is a function of the position in the shock. The instability properties are unchanged and depend only on the relative drift velocity $\underset{\sim}{U} = \underset{\sim}{V}_d - \underset{\sim}{V}_u$ (which is independent of the position in the shock) and $\eta(z)$ (which is dependent on the position in the shock). It is convenient, at this stage, to specify all the properties and criteria in terms of the upstream Alfven Mach number $M_A = V_u/C_{A0}$ and the fraction $\zeta$ of the distance through the shock. From (1), we have

$$n_e(z) = (1 - \zeta)\, n_{u\infty} + \zeta\, n_{d\infty} \tag{12}$$

where $n_{u\infty}$ and $n_{d\infty}$ represent respectively the uptstream and downstream densities at infinity. Thus

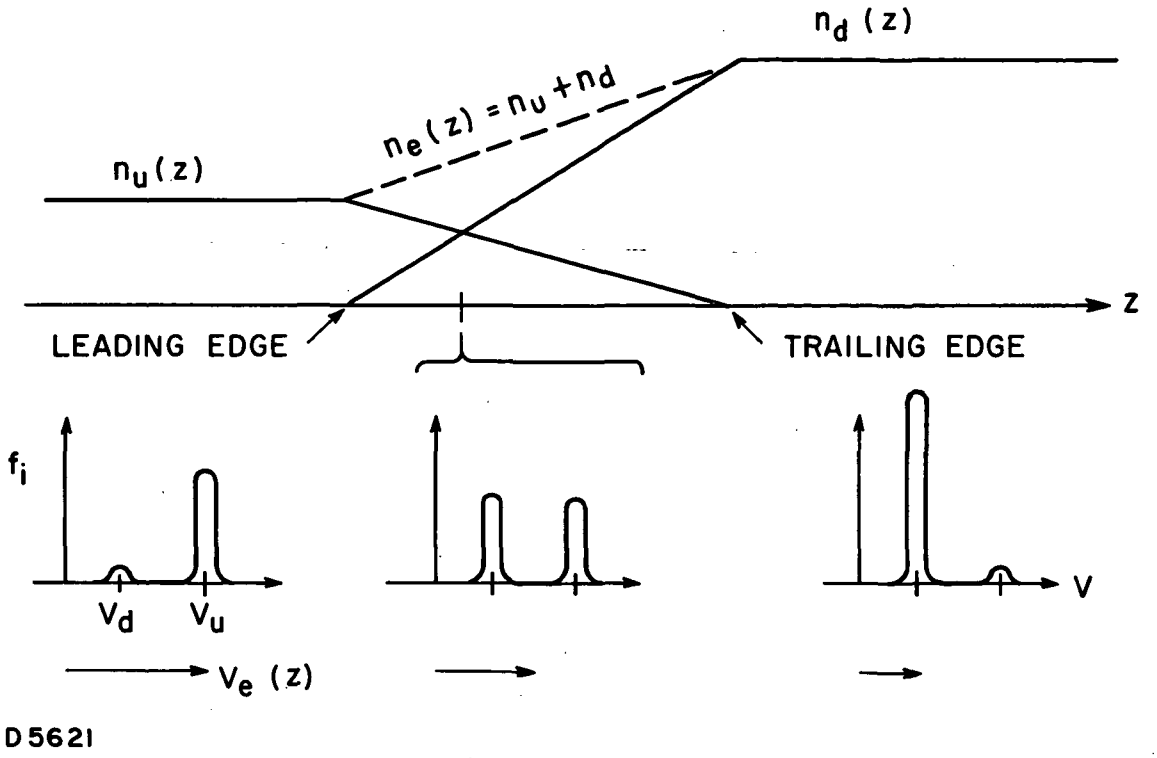


Fig. 5 Sketch of the Ion Velocity Distribution Function Indicating the Assumed Linear Variation Through the Shock.

$$\zeta = \frac{\eta}{\eta + \tau\ (1 - \eta)} \tag{13}$$

where $\tau$ is the compression ratio across the shock which can be obtained from the Rankine-Hugoniot relations (with $C_{S0} = C_{A0}$) as

$$\tau = \frac{(\gamma + 1)\ M_A^2}{(\gamma - 1)\ M_A^2 + 2} = \frac{4M_A^2}{M_A^2 + 3} \quad (\text{for } \gamma = 5/3). \tag{14}$$

The local Alfven velocity decreases through the shock as the plasma density increases and is given by

$$C_A = C_{A0} \left[ \frac{M_A^2 + 3}{M_A^2 + 3 + 3\zeta\ (M_A^2 - 1)} \right]^{1/2} \tag{15}$$

while the local drift Mach number $M_d$ is

$$M_d = \frac{V_u - V_d}{C_A} = \frac{3(M_A^2 - 1)}{4M_A^2} \left[ 1 + \frac{3\zeta\ (M_A^2 - 1)}{M_A^2 + 3} \right]^{1/2} \tag{16}$$

With the help of (11) to (16), the dispersion relation in the shock frame can be written as

$$\omega_s^3 + a\,(k)\ \omega_s^2 + b\,(k)\ \omega_s + c\,(k) = 0$$

where

$$\omega_s = \omega + \underset{\sim}{k} \cdot \underset{\sim}{V}_e\,(z)$$

and a, b, and c, are known functions of k, $M_A$ and $\zeta$. The group velocity of the wave $\partial \omega'_s / \partial k$ where $\omega'_s$ is the real part of $\omega_s$ is given by

$$\partial\omega'_s\ /\ \partial k = - \frac{8\omega'^2_s \frac{\partial a}{\partial k} + 2\omega'_s \frac{\partial (a^2 + b)}{\partial k} + \frac{\partial (a\ b - c)}{\partial k}}{24\omega'^2_s + 16\ a\ \omega'_s + 2(a^2 + b)} \tag{17}$$

for the unstable modes.

The unstable regions in k - $M_A$ space are as before easily obtained by setting the discriminant of (17) equal to zero. These are presented in Figs. 6a and 6b for two different values of $\zeta$. These figures are different from Figs. 4a and 4b since the value of $\eta$ varies for different values of $M_A$ for constant $\zeta$. We see that near the front of the shock there is a wide range of unstable wave numbers for $M_A \gtrsim 3$. The growth rate is of the order $\Omega_{ci}$. However, most of these waves have positive group velocities and are swept downstream with the flow before they have had a chance to grow significantly. Only unstable waves with nearly zero group velocity can be expected to grow to large amplitude. In Fig. 6a, the values of k for zero group velocity waves in the unstable region are shown by a dashed line. Thus, Mach numbers in the range $6.8 < M_A < 9.1$ should be able to produce turbulence at $\zeta \geq 0.05$ according to the linearized analysis presented here. Such waves do not exist for the parameter ranges shown in Fig. 6b at $\zeta \geq 0.2$.

Figure 7 shows the range of upstream Alfven Mach numbers for which unstable whistlers will stand in the shock as a function of distance into the shock. Two immediate conclusions can be made. The first is that the mechanism can be important only for $M_A > 5.5$. The second is that these waves are confined to the leading edge of the shock; unstable waves near the middle or trailing edge will be swept downstream. This result is in agreement with laboratory experiments[13] that measured magnetic field fluctuations in lower Mach number shock waves.

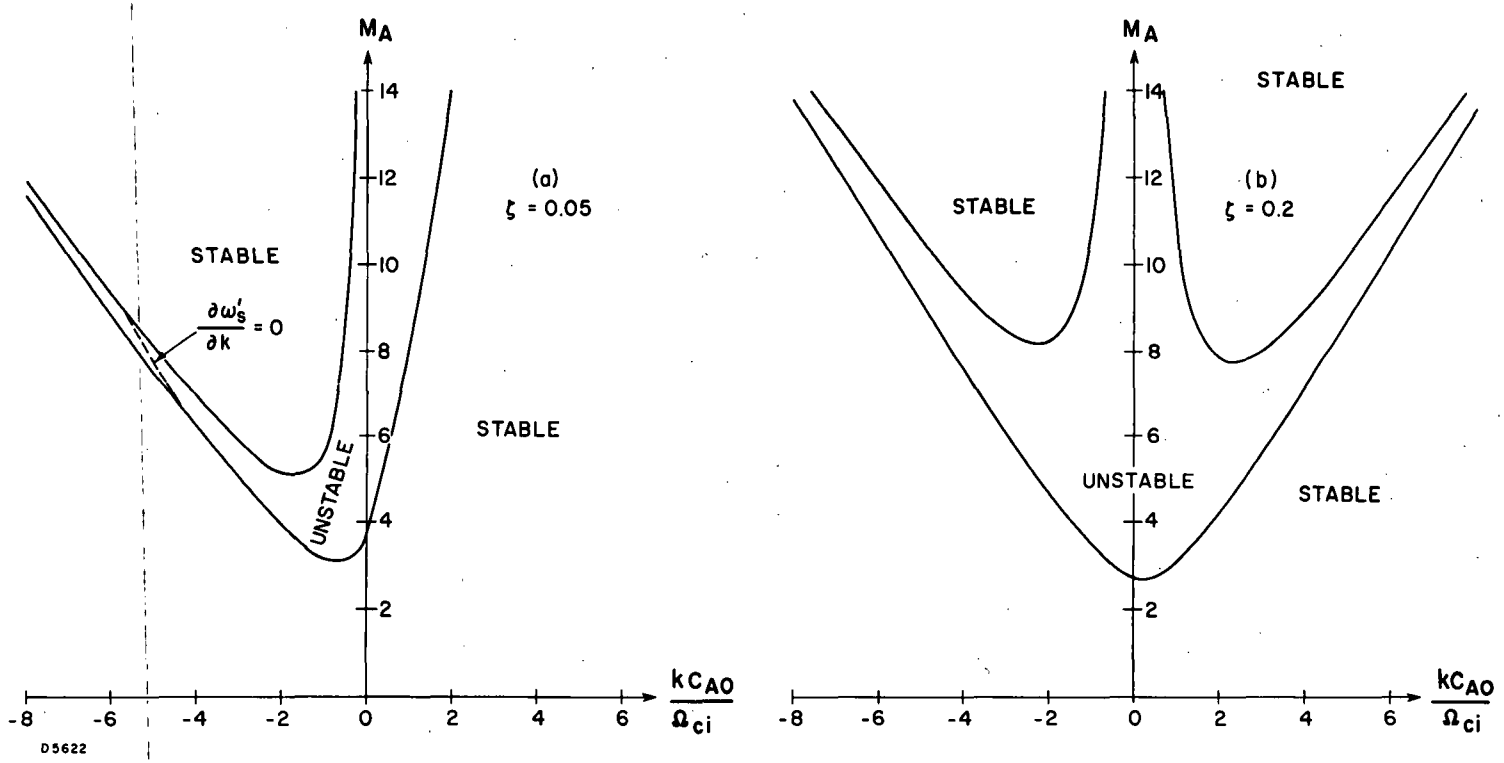


Fig. 6 Range of Unstable Wave Numbers as a Function of Upstream Alfven Mach number at Two Positions Within the Shock Front at a) $\zeta = 0.05$ and b) $\zeta = 0.2$. The dashed line corresponds to values of k for which the group velocity of unstable waves is zero in the shock front.

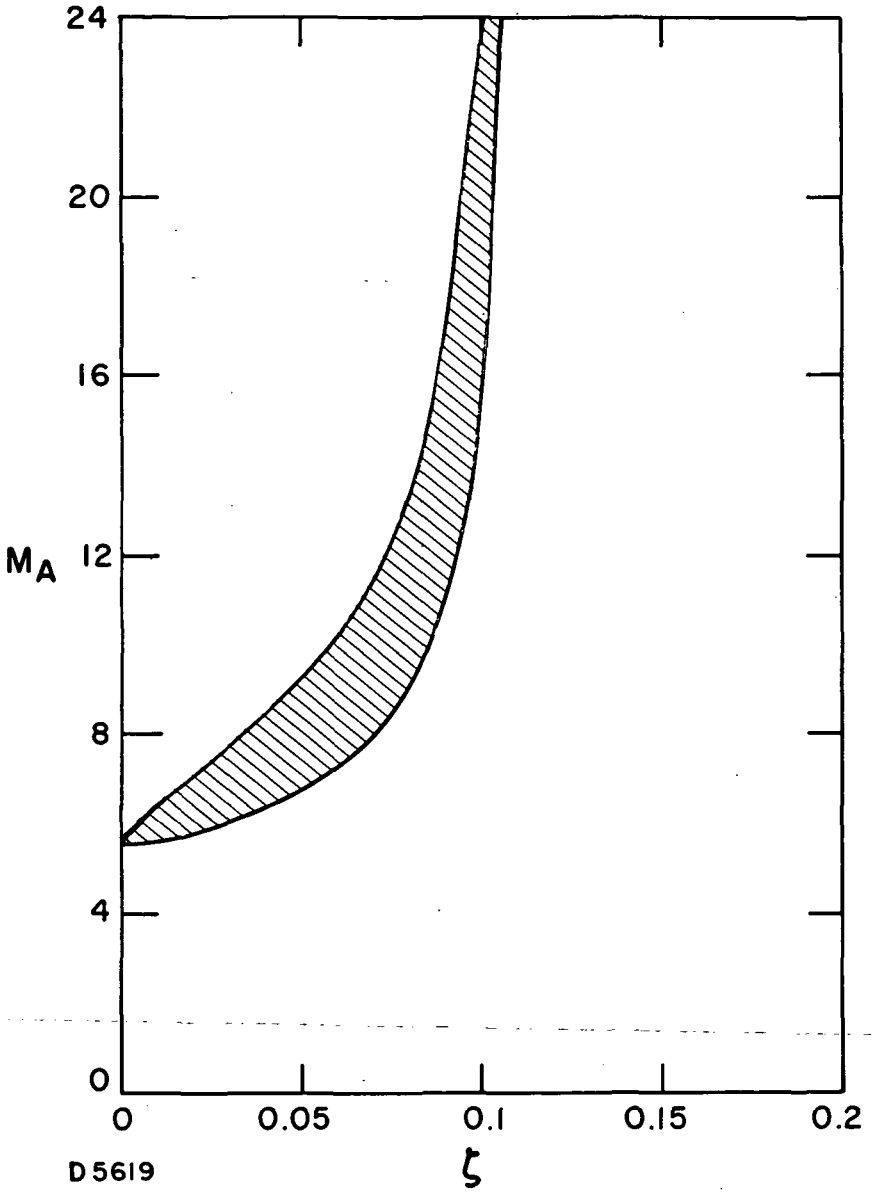


Fig. 7 Range of Alfven Mach Numbers for Which Unstable Whistlers Will Stand in the Shock as a Function of Position Within the Shock.

## SUMMARY

We have derived the electromagnetic dispersion relation for two counterstreaming ion beams in a stationary electron background. The dispersion relation which is unaffected by electron pressure terms in the fluid approximation has been solved numerically to find the regions of instability in k - $M_d$ space. It is found that for beam-whistler modes to be unstable, it is necessary that the relative drift Mach number be greater than 2.0 although this condition is not sufficient for instability. The bandwidth of k over which the unstable modes exist is shown to decrease inversely with the relative drift velocity for large relative drift velocities.

By modeling the shock structure in a Mott-Smith formalism as consisting of streaming upstream and downstream ions, the linear analysis was applied to the study of shock wave structure propagating along the magnetic field. Invoking the criterion that only unstable waves with zero group velocity will have time to grow within the shock thickness, we found the range of Mach numbers for which some unstable beam-whistler modes could grow to large amplitudes. We suggest that this may be a possible mechanism to generate turbulence that many experiments have shown to be associated with shock wave structures. The plasma turbulence in turn can provide the explanation for anomalous dissipation. However, in our model, the unstable beam-whistler modes can stand near the leading edge of the shock only for upstream Mach

numbers greater than 5.5.

The most serious limitation of the present analysis is the restriction $\underset{\sim}{k} \parallel \underset{\sim}{B}_o$. For waves propagating at an angle to the magnetic field, the dispersion relation becomes much more complicated and electron thermal effects have a significant interaction with the magnetic modes treated here. The analysis presented here ought to be extended to include the stability properties of these obliquely propagating waves. The assumption of cold ions ought to be relaxed particularly since one of the ion species in this study has been taken to be the shocked ions. Ion thermal effects could have a significant effect on the stability properties of counter-streaming ion beams. The results of the stability analysis for hot streaming plasmas will be reported later. As a final comment, it should be emphasized that this instability depends on having included the effect of the magnetic field on the ions. If $\Omega_{ci} \to 0$ in (4), the instability disappears.

## REFERENCES


1. J. D. Jackson, Plasma Phys. (J. Nucl. Energy, Part C) 1, 171 (1960).

2. T. E. Stringer, J. Nucl. Energy, Part C, 6, 267 (1964).

3. K. Papadopoulos, R. C. Davidson, J. M. Dawson, I. Haber, D. A. Hammer, N. A. Krall, and R. Shanny, Phys. Fluids 14, 849 (1971).

4. R. W. Landau, Phys. Fluids 15, 1991 (1972).

5. J. B. McBride and E. Ott, Electromagnetic and Finite $\beta_e$ Effects on the Modified Two-Stream Instability, NRL Memorandum Report 2366 (October, 1971).

6. J. B. McBride, E. Ott, J. P. Boris and J. H. Orens, Phys. Fluids 15, 2367 (1972).

7. M. Lampe, W. M. Manheimer, J. B. McBride, K. Papadopoulos, J. H. Orens, R. Shanny, and R. N. Sudan, Phys. Fluids 15, 662 (1972).

8. D. Forslund, R. Morse, C. Nielson and J. Fu, Phys. Fluids, 15, 1303 (1972).

9. D. Biskamp and H. Welter, J. Geophys, Res. 77, 6052 (1972).

10. R. L. Briggs, "Electron-Stream Interaction with Plasmas," (MIT Press, Cambridge, Massachusetts 1964), p. 83.

11. M. S. Kovner, Soviet Phys. JETP 13, 369 (1961).

12. A. R. Kantrowitz and H. E. Petschek, "MHD Characteristics and Shock Waves in Plasma Physics in Theory and Application," (ed. W. B. Kunkel, McGraw-Hill Co., New York, 1966) pp. 148-206.

13. R. M. Patrick and E. R. Pugh, Phys. Fluids 12, 366 (1969).